

## Quark and Glue Momenta and Angular Momenta in the Proton — a Lattice Calculation

---

**K.F. Liu<sup>\* a</sup>, M. Deka<sup>b,c</sup>, T. Doi<sup>d</sup>, Y.B. Yang<sup>e</sup>, B. Chakraborty<sup>a</sup>, Y. Chen<sup>e</sup>, S.J. Dong<sup>a</sup>, T. Draper<sup>a</sup>, M. Gong<sup>a</sup>, H.W. Lin<sup>f</sup>, D. Mankame<sup>a</sup>, N. Mathur<sup>g</sup>, and T. Streuer<sup>b</sup>**

<sup>a</sup>Department of Physics and Astronomy, University of Kentucky, Lexington, KY 40506

<sup>b</sup>Institute for Theoretical Physics, University of Regensburg, 93040 Regensburg, Germany

<sup>c</sup>The Institute of Mathematical Sciences, Chennai 6000113, India

<sup>d</sup>Theoretical Research Division, Nishina Center, RIKEN, Wako 351-0198, Japan

<sup>e</sup>Institute of High Energy Physics, Chinese Academy of Sciences, Beijing 1000190, China

<sup>f</sup>Department of Physics, University of Washington, Seattle, WA 98195

<sup>g</sup>Department of Theoretical Physics, Tata Institute of Fundamental Research, Mumbai 40005, India

E-mail: [liu@pa.uky.edu](mailto:liu@pa.uky.edu)

( $\chi$ QCD Collaboration)

We report a complete calculation of the quark and glue momenta and angular momenta in the proton. These include the quark contributions from both the connected and disconnected insertions. The calculation is carried out on a  $16^3 \times 24$  quenched lattice at  $\beta = 6.0$  and for Wilson fermions with  $\kappa = 0.154, 0.155$ , and  $0.1555$  which correspond to pion masses at 650, 538, and 478 MeV. The quark loops are calculated with  $Z_4$  noise and signal-to-noise is improved further with unbiased subtractions. The glue operator is comprised of gauge-field tensors constructed from the overlap operator. The  $u$  and  $d$  quark momentum/angular momentum fraction is  $0.66(5)/0.72(5)$ , the strange momentum/angular momentum fraction is  $0.024(6)/0.023(7)$ , and that of the glue is  $0.31(6)/0.25(8)$ . The orbital angular momenta of the quarks are obtained from subtracting the quark spins from the corresponding angular momentum components. As a result, the quark orbital angular momentum constitutes  $0.50(2)$  of the proton spin, with almost all of it coming from the disconnected insertion. The quark spin carries a fraction  $0.25(12)$  and glue carries a fraction  $0.25(8)$  of the total proton spin.

*XXIX International Symposium on Lattice Field Theory*

*July 10-16 2011*

*Squaw Valley, Lake Tahoe, California*

---

\*Speaker.

## 1. Introduction

Determining the contributions of quarks and gluons to the nucleon spin is one of the challenging issues in QCD both experimentally and theoretically. Since the contribution from the quark spin is small ( $\sim 25\%$ ) from deep inelastic scattering experiments, it is expected that the rest should come from glue spin and the orbital angular momenta of quarks and glue.

Lattice calculations of the quark orbital angular momenta have been carried out for the connected insertions [1, 2, 3, 4] and it was shown to be small [1] in the quenched calculation and near zero in dynamical fermion calculations [2, 3, 4] due to the cancellation between those of the  $u$  and  $d$  quarks. Gluon helicity distribution  $\Delta G(x)/G(x)$  from both COMPASS and STAR experiments is found to be close to zero [5]. Furthermore, it is argued based on analysis of single-spin asymmetry in unpolarized lepton scattering from a transversely polarized nucleon that the glue orbital angular momentum is absent [6]. Thus, it appears that we have encountered a ‘Dark Spin’ scenario.

In this work, we give a complete calculation of the quark and glue momenta and angular momenta. The quark contributions in both the connected and disconnected insertions are included. Combining with earlier work of the quark spin, we obtain the quark orbital angular momenta. We find that indeed the  $u$  and  $d$  quark orbital angular momenta largely cancel in the connected insertion. However, their contributions including the strange quark are large (50%) in the disconnected insertion due to the fact that the quark spin for each of the  $u$ ,  $d$ , and  $s$  quarks in the disconnected insertion is large and negative. We have been able to obtain the glue momentum and angular momentum for the first time, mainly because the overlap operator is used for the gauge-field tensor which is less noisy than that constructed from the gauge links. The lattice renormalization of the quark and glue energy-momentum operators are achieved through the momentum and angular momentum sum rules. Due to these sum rules, the gravitomagnetic moment is zero as proven for composite systems from the light-cone Fock representation [7].

## 2. Formalism

### 2.1 Angular Momenta and Momenta for Quarks and Gluons

The angular momentum operator in QCD can be expressed as a gauge-invariant sum [8],

$$\vec{J}_{\text{QCD}} = \vec{J}_q + \vec{J}_g = \frac{1}{2}\vec{\Sigma} + \vec{L}_q + \vec{J}_g \quad (2.1)$$

where  $\vec{J}_q = \frac{1}{2}\vec{\Sigma} + \vec{L}_q$  and  $\vec{J}_g$  are the quark and gluon contributions respectively.  $\vec{\Sigma}$  is the quark spin operator, and  $\vec{L}_q$  is the quark orbital angular momentum operator.  $\vec{J}_{q,g}$  can be expressed in terms of the energy-momentum tensor operator through

$$J_i^{q,g} = \frac{1}{2} \epsilon_{ijk} \int d^3x (\mathcal{T}_{4k}^{q,g} x^j - \mathcal{T}_{4j}^{q,g} x^k) \quad (2.2)$$

Similarly, the quark and glue momentum operators are

$$P_i^{q,g} = \int d^3x \mathcal{T}_{4i}^{q,g}, \quad (2.3)$$

where

$$\mathcal{T}_{4i}^q = \frac{-i}{4} \sum_f \bar{\Psi}_f [\gamma_4 \vec{D}_i + \gamma_i \vec{D}_4 - \gamma_4 \overleftarrow{D}_i - \gamma_i \overleftarrow{D}_4] \Psi_f \quad (2.4)$$

and

$$\mathcal{T}_{4i}^g = i \sum_{k=1}^3 G_{4k} G_{ki} \quad (2.5)$$

The matrix element of the energy-momentum tensor,  $\mathcal{T}_{4i}$ , between two nucleon states with momenta,  $p'$  and  $p$ , can be written as [8] (in Euclidean space),

$$\begin{aligned} \langle p, s | \mathcal{T}_{4i}^{q,g} | p', s' \rangle &= \left( \frac{1}{2} \right) \bar{u}(p, s) \left[ T_1(q^2) (\gamma_4 \bar{p}_i + \gamma_i \bar{p}_4) - \frac{1}{2m} T_2(q^2) (\bar{p}_4 \sigma_{i\alpha} q_\alpha + \bar{p}_i \sigma_{4\alpha} q_\alpha) \right. \\ &\quad \left. - \frac{i}{m} T_3(q^2) q_4 q_i \right]_{q,g} u(p', s') \end{aligned} \quad (2.6)$$

where,  $\bar{p} = \frac{1}{2}(p + p')$ ,  $q_\mu = p_\mu - p'_\mu$ ,  $m$  is the mass of the nucleon, and  $u(p, s)$  is the nucleon spinor.

By substituting Eq. (2.6) into Eqs. (2.2) and (2.3) at  $q^2 \rightarrow 0$  limit, one obtains

$$J_{q,g} = \frac{1}{2} [T_1(0) + T_2(0)]_{q,g}, \quad (2.7)$$

$$\langle x \rangle_{q,g} = T_1(0)_{q,g}. \quad (2.8)$$

In this present study, there are two operators — energy momentum tensors for the quarks and glue. We can use the momentum and angular momentum sum rules to perform the renormalization on the lattice

$$Z_q(a) T_1(0)_q + Z_g(a) T_1(0)_g = 1, \quad (2.9)$$

$$Z_q(a) [T_1(0)_q + T_2(0)_q] + Z_g(a) [T_1(0)_g + T_2(0)_g] = 1. \quad (2.10)$$

After the lattice renormalization, one can perform perturbative mixing and matching to the  $\overline{\text{MS}}$  scheme at  $\mu = 2$  GeV.

It is interesting to note that from these equations, i.e. Eqs. (2.9) and (2.10), one obtains the sum of the  $T_2(0)$ 's for the quarks and glue to be zero, i.e.

$$Z_q(a) T_2(0)_q + Z_g(a) T_2(0)_g = 0. \quad (2.11)$$

This shows that the total anomalous gravitomagnetic moment of the nucleon vanishes. This has been proven by Brodsky *et al.* [7] for composite systems from the light-cone Fock representation and now it is shown as a consequence of momentum and angular momentum conservation. We will see how large the individual quark and glue contributions are.

Since  $T_1(q^2)$  and  $T_2(q^2)$  can have different  $q^2$  behaviors, we shall compute them separately at different  $q^2$  values [2], and then separately extrapolate them to  $q^2 \rightarrow 0$  for both the quark and glue contributions.

## 2.2 Glue Energy-Momentum Tensor Operator

It is well-known that gauge operators from the link variables are quite noisy. We adopt the glue energy-momentum tensor operator where the field tensors are obtained from the overlap Dirac operator. The gauge-field tensor has been derived from the massless overlap operator  $D_{\text{ov}}$  [9]

$$\text{Tr}_s [\sigma_{\mu\nu} D_{\text{ov}}(x, x)] = c_T a^2 G_{\mu\nu}(x) + \mathcal{O}(a^3) \quad (2.12)$$

where  $\text{Tr}_s$  is the trace over spin.  $c_T = 0.11157$  for  $\kappa = 0.19$ . With this construction, we expect the ultraviolet fluctuations to be suppressed, since  $D_{\text{ov}}$  is exponentially local and  $D_{\text{ov}}(x, x)$  involves gauge loops beginning and ending at  $x$ , which serves as smearing.

## 3. Lattice Calculations and Numerical Parameters

In order to obtain  $J_{q,g} = \frac{1}{2} [T_1(0) + T_2(0)]_{q,g}$  and  $\langle x \rangle_{q,g} = T_1(0)_{q,g}$ , we first calculate the three-point functions,  $G_{N\mathcal{F}_{4iN}}(\vec{p}, t_2; \vec{q}, t_1; \vec{p}', t_0)$  and the two-point functions  $G_{NN}(\vec{p}, t_2)$ . Here  $\vec{p}$  is the sink momentum,  $\vec{q}$  is the momentum transfer, and  $\vec{p}'$  is the source momentum.  $t_0$ ,  $t_1$  and  $t_2$  are the source, current insertion, and sink time respectively. We then take the following ratios between three-point and two-point functions, which involve the combinations of  $T_1(q^2)$ ,  $T_2(q^2)$ , and  $T_3(q^2)$

$$\frac{\text{Tr} [\Gamma_{e,m} G_{N\mathcal{F}_{4iN}}(\vec{p}, t_2; -\vec{q}, t_1; \vec{p}', t_0)]}{\text{Tr} [\Gamma_e G_{NN}(\vec{p}, t_2)]} \times \sqrt{\frac{\text{Tr} [\Gamma_e G_{NN}(\vec{p}', t_2 - t_1 + t_0)]}{\text{Tr} [\Gamma_e G_{NN}(\vec{p}, t_2 - t_1 + t_0)]}} \times \sqrt{\frac{\text{Tr} [\Gamma_e G_{NN}(\vec{p}, t_1)]}{\text{Tr} [\Gamma_e G_{NN}(\vec{p}', t_1)]} \cdot \frac{\text{Tr} [\Gamma_e G_{NN}(\vec{p}, t_2)]}{\text{Tr} [\Gamma_e G_{NN}(\vec{p}', t_2)]}}}_{t_1 \gg t_0, t_2 \gg t_1} \frac{[a_1 T_1(q^2) + a_2 T_2(q^2) + a_3 T_3(q^2)]}{4\sqrt{E_p(E_p + m)E_{p'}(E_{p'} + m)}} \quad (3.1)$$

where  $\Gamma_m = (-i)/2(1 + \gamma_4)\gamma_m\gamma_5$  is the spin polarized projection operator, and  $\Gamma_e = 1/2(1 + \gamma_4)$  is the unpolarized projection operator. For the special case with  $\vec{p} = 0$ , one obtains the combination of  $[T_1 + T_2](q^2)$

$$\frac{\text{Tr} [\Gamma_m G_{N\mathcal{F}_{4iN}}(\vec{0}, t_2; -\vec{q}, t_1; \vec{p}', t_0)]}{\text{Tr} [\Gamma_e G_{NN}(\vec{0}, t_2)]} \cdot \frac{\text{Tr} [\Gamma_e G_{NN}(\vec{0}, t_1)]}{\text{Tr} [\Gamma_e G_{NN}(-\vec{q}, t_1)]} \Big|_{t_1 \gg t_0, t_2 \gg t_1} \varepsilon_{ijm} q_j [T_1 + T_2](q^2), \quad (3.2)$$

and the forward matrix element, which is obtained with the following ratio

$$\frac{\text{Tr} [\Gamma_e G_{N\mathcal{F}_{4iN}}(\vec{p}, t_2; \vec{0}, t_1; \vec{p}, t_0)]}{|\vec{p}| \text{Tr} [\Gamma_e G_{NN}(\vec{p}, t_2)]} \Big|_{t_1 \gg t_0, t_2 \gg t_1} \langle x \rangle. \quad (3.3)$$

Since the quark  $T_1(q^2)$  and  $T_2(q^2)$  for the connected insertion are shown to have quite different  $q^2$  behavior [2, 3, 4], we will need to separately extrapolate  $T_1(q^2)$  and  $T_2(q^2)$  to  $q^2 \rightarrow 0$ . We combine several kinematics and with both the polarized and unpolarized three-point functions to extract  $T_1(q^2)$ ,  $T_2(q^2)$ , and  $T_3(q^2)$  which appear as different combinations in the 3-point to 2-point ratios in Eqs. (3.1) and then extrapolate  $T_1(q^2)$  and  $T_2(q^2)$  in  $q^2$  to obtain  $T_1(0)$  and  $T_2(0)$ . We can check this by comparing the extracted  $T_1(q^2) + T_2(q^2)$  against the  $[T_1 + T_2](q^2)$  obtained directly from Eqs. (3.2) and (3.3) at comparable  $q^2$ .

The three-point functions for quarks have two topologically distinct contributions in the path-integral diagrams — one from connected (CI) and the other from disconnected insertions (DI) [10, 11, 12]. For DI, we sum over the current insertion time,  $t_1$ , between the source and the sink time, i.e. from  $t_1 = t_0 + 1$  to  $t_2 - 1$  [13, 14, 15, 16] in order to increase the statistics. Similarly for the glue. Then the corresponding ratios at large time separation for Eqs. (3.1), (3.2), and (3.3) are  $\frac{[a_1 T_1(q^2) + a_2 T_2(q^2) + a_3 T_3(q^2)]}{4\sqrt{E_p(E_p+m)E_{p'}(E_{p'}+m)}} \times t_2 + \text{const.}$ ,  $\varepsilon_{ijm} q_j [T_1 + T_2](q^2)_{q,g} \times t_2 + \text{const.}$ , and  $\langle x \rangle \times t_2 + \text{const.}$  respectively.

We then extract the slopes and obtain  $T_1(0)$ ,  $T_2(0)$ ,  $[T_1 + T_2](q^2)_{q,g}$  and  $\langle x \rangle_{q,g}$  in the DI the same way as was done for the CI.

We use 500 gauge configurations on a  $16^3 \times 24$  lattice generated with Wilson action at  $\beta = 6.0$  in the quenched approximation. The values of the hopping parameter we use are  $\kappa = 0.154, 0.155$ , and  $0.1555$ . The critical hopping parameter,  $\kappa_c = 0.1568$  is obtained by a linear extrapolation to the zero pion mass [17]. Using the nucleon mass to set the lattice spacing at  $a = 0.11$  fm, the corresponding pion masses are 650(3), 538(4), and 478(4) MeV, and the nucleon masses are 1291(9), 1159(11), and 1093(13) MeV, respectively. We use Dirichlet boundary condition in the present work.

In the case of DI, the quark loop is evaluated separately. We compute it stochastically by using complex  $Z_2$  noise vector [18]. The number of noise vectors we use is 500 on each gauge configuration. Also for the case of quarks, we shall define two  $\kappa$ 's for the quark mass:  $\kappa_v$  for valence quarks, and  $\kappa_{\text{sea}}$  for sea quarks. For the strange quark current, we have fixed  $\kappa_{\text{sea}} = 0.154$  which is close to the strange quark mass as determined from the  $\phi$  meson mass, and  $\kappa_v$  takes the values of 0.154, 0.155, and 0.1555. For up and down quarks, we consider the cases with equal valence and sea quark masses, i.e.  $\kappa_{\text{sea}} = \kappa_v = 0.154, 0.155$ , and  $0.1555$ .

In the case of glue, we construct the energy-momentum tensor from the gauge field tensors which are calculated from the massless overlap operator,  $D_{\text{ov}}$  [9, 19] as discussed in Sec. 2.2.  $D_{\text{ov}}(x, x)$  at all space-time points are estimated stochastically where we compute the color and spin indices exactly, but we perform space-time dilution by a separation of two sites on top of odd/even dilution. Therefore, the “taxi-driver distance” = 4 in our case. We use two  $Z_4$  noise sources, and take the average of them on each configuration.

Due to the stochastic estimation, there is noise in addition to that from the gauge configurations. So, we adopt the following techniques to reduce the error:

- We use discrete symmetries to discard the unwanted part of the current and the two-point functions when we correlate the current to the two-point functions to construct the three-point functions [20, 21, 1]. Combining  $\gamma_5$ -Hermiticity, parity and  $CH$  transformation, we determine whether the real or imaginary part of the current and the two-point functions will contribute to the three-point functions.
- We employ unbiased subtraction to the noise estimation of the quark loop to reduce the contributions from the off-diagonal matrix elements [22, 1, 15]. We use four subtraction terms ( $\kappa D$ ,  $\kappa^2 D^2$ ,  $\kappa^3 D^3$  and  $\kappa^4 D^4$ ). No subtraction has been implemented for the estimation of the glue matrix elements.

- We use multiple nucleon sources (in our case, 16) to increase the statistics. We correlate the nucleon propagators at different source locations with the already computed quark loops which results in significant reduction of errors [15, 16].

The error analysis is performed by using the jackknife procedure. The correlation among different quantities are taken into account by constructing the corresponding covariance matrices. In order to extract various physical quantities, we use correlated least- $\chi^2$  fits.

#### 4. Numerical Results

We first present our results of the CI. In Fig. 1(a), we plot  $T_{1,u}(q^2) + T_{2,u}(q^2)$  and  $T_{1,d}(q^2) + T_{2,d}(q^2)$  as a function of  $-q^2$  for the case of  $\kappa = 0.1555$ , where  $T_1(q^2)$  and  $T_2(q^2)$  are obtained from Eq. (3.1). We also plot  $[T_{1,u} + T_{2,u}](q^2)$  and  $[T_{1,d} + T_{2,d}](q^2)$  directly from Eq. (3.2) at slightly different  $-q^2$ . We see that the latter basically agrees with the error band of the former with a dipole fit in  $-q^2$  within 2 sigmas. This is a cross check of our procedure of extracting  $T_1(q^2)$  and  $T_2(q^2)$  from Eq. (3.1) which involves 3 to 4 equations of the combinations of  $T_1(q^2)$ ,  $T_2(q^2)$ , and  $T_3(q^2)$  at different  $q^2$ . We also show, in Fig. 1(b),  $T_{1,u}(q^2) + T_{1,d}(q^2)$  and  $T_{2,u}(q^2) + T_{2,d}(q^2)$  and their error bands. Also plotted is  $T_{1,u}(0) + T_{1,d}(0)$  from Eq. (3.3). We see that its error is smaller than that from the separately extrapolated  $T_{1,u}(0)$  and  $T_{1,d}(0)$ . Thus we shall use  $T_{1,u}(0) + T_{1,d}(0)$  from Eq. (3.3) and combine with  $T_{2,u}(q^2) + T_{2,d}(q^2)$  to get the angular momentum for the CI.

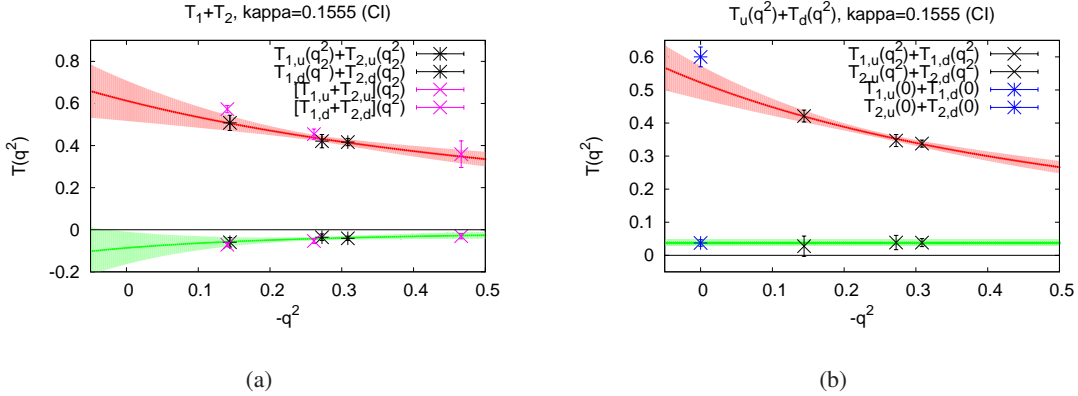


**Figure 1:** Results from  $\kappa = 0.1555$ : (a) The sum of  $T_1(q^2)$  and  $T_2(q^2)$  extracted from Eq. (3.1) with error bands from the dipole fit is compared to  $[T_1 + T_2](q^2)$  from Eq. (3.2) with slightly different  $-q^2$  for  $u$  and  $d$  quarks in the CI. (b) The sum of  $u$  and  $d$  quark contributions for  $T_1(q^2)$  and  $T_2(q^2)$ . The blue asterisk at  $-q^2 = 0$  is  $T_{1,u}(0) + T_{1,d}(0)$  from Eq. (3.3).

For the DI with  $\kappa_v = \kappa_{\text{sea}} = 0.1555$  at  $q^2 a^2 = -0.144$ , we show in Fig. 2(a) the ratio of Eq. (3.2) with  $t_1$  summed between  $t_0 + 1$  and  $t_2 - 1$  and plotted against the sink time  $t_2$  so that the slope is  $\epsilon_{ijm} q_j [T_1 + T_2](q^2)$ . We fit the slope from  $t_2 = 8$  where the ratio is dominated by the nucleon to  $t_2 = 12$ . We plot  $[T_1 + T_2](q^2)$  so obtained in Fig. 2(b) and compare them to  $T_1(q^2) + T_2(q^2)$  extracted from 5 to 6 combinations of  $a_1 T_1(q^2) + a_2 T_2(q^2) + a_3 T_3(q^2)$ . We see that they are consistent with each other within errors. The error bands are from the dipole fits of  $T_1(q^2)$  and  $T_2(q^2)$ .  $T_1(0)$  (red square) is from the forward matrix element which has smaller error than the  $-q^2$  extrapolated

$T_1(0)$ . We shall combine it with the extrapolated  $T_2(0)$  for the angular momentum  $J$  in the DI. Finally, we perform a linear chiral extrapolation to obtain  $T_1(0) + T_2(0)$  for the  $u/d$  quark at the chiral limit. This is shown in Fig. 2(c). For the strange, we fix the quark loop at  $\kappa_{\text{sea}} = 0.154$  and extrapolate  $\kappa_r$  to the chiral limit.

We perform similar analysis for the glue momentum and angular momentum. They are plotted in Figs. 3(a), 3(b) and 3(c).

With all the quark and glue momenta and angular momenta, we carry out lattice renormalization through the sum rules in Eqs. (2.9) and (2.10). We obtain  $Z_q(a) = 1.05$  and  $Z_g(a) = 1.05$ . This shows that both the lattice operators, particularly the glue energy-momentum tensor from the overlap operator, are ‘natural’ and close to the continuum. In Table 1, we list the quark momentum fractions  $\langle x \rangle = T_1(0)$  in the CI ( $u$  and  $d$ ) and the DI ( $u/d$  and  $s$ ) and that of the glue. We also list the corresponding  $T_2(0)$  and angular momentum  $2J = T_1(0) + T_2(0)$ .

**Table 1:** Lattice renormalized values with renormalization constants  $Z_q=Z_g=1.05$ .

	CI( $u$ )	CI( $d$ )	CI( $u+d$ )	DI( $u/d$ )	DI( $s$ )	Glue
$\langle x \rangle$	0.428(40)	0.156(20)	0.586(45)	0.038(7)	0.024(6)	0.313(56)
$T_2(0)$	0.297(112)	-0.228(80)	0.064(22)	-0.002(2)	-0.001(3)	-0.059(52)
$2J$	0.726(118)	-0.072(82)	0.651(50)	0.036(7)	0.023(7)	0.254(76)
$g_A$	0.91(11)	-0.30(12)	0.61(8)	-0.12(1)	-0.12(1)	—
$2L$	-0.18(16)	0.23(15)	0.04(9)	0.16(1)	0.14(1)	—

We see from Table 1 that the strange momentum fraction  $\langle x \rangle_s = 0.024(6)$  is in the range of uncertainty of  $\langle x \rangle_s$  from the CTEQ fitting of the parton distribution function from experiments which is  $0.018 < \langle x \rangle_s < 0.040$  [23]. The glue momentum fraction of 0.313(56) is smaller than, say, the CTEQ4M fit of 0.42 at  $Q = 1.6$  GeV [24]. We expect the glue momentum fraction to be larger than the present result when dynamical configurations with light fermions are used in the calculation. From Figs. 1(b) and 3(b) and Table 1, we find that the central values of  $T_2(0)$  for  $u/d$  and  $s$  in the DI are small and consistent with zero.  $T_{2,u}(0) + T_{2,d}(0)$  in CI is positive, while  $T_{2,g}(0)$  is negative. With the renormalization constants  $Z_q(q)$  and  $Z_g(a)$  fitted to be both positive (and near unity), they cancel giving a null anomalous gravitomagnetic moment. The fact that their unrenormalized magnitudes are almost identical is consistent with the finding that  $Z_q(q)$  and  $Z_g(a)$  are the same in size within errors.

In analogy to  $F_2(0)$  which is known as the anomalous magnetic moment of the nucleon,  $T_2(0)$  is termed the anomalous gravitomagnetic moment and has been shown by Brodsky *et al.* to vanish for composite systems [7]. We have now verified that this is the consequence of the momentum and angular momentum sum rules.

The flavor-singlet  $g_A^0$ , which is the quark spin contribution to the nucleon, has been calculated before on the same lattice [14]. We can subtract it from the total angular momentum fraction  $2J$  to obtain the orbital angular momentum fraction  $2L$  for the quarks. As we see in Table 1, the orbital angular momentum fractions  $2L$  for the  $u$  and  $d$  quarks in the CI have different signs and they add up close to zero, 0.04(9). This is the same pattern seen with dynamical fermions configurations

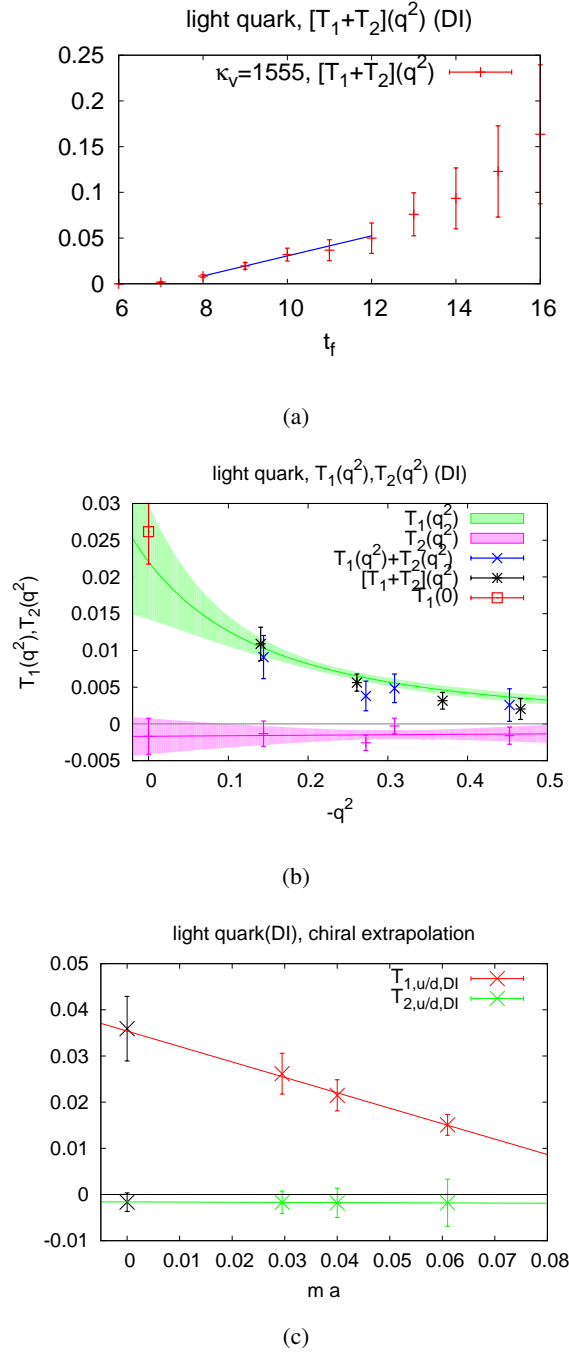


**Figure 2:** (a) The ratio of Eq. (3.2) with  $t_1$  summed between  $t_0 + 1$  and  $t_2 - 1$  as a function of the sink time  $t_2$ . The slope is fitted to obtain  $\varepsilon_{ijm}q_j [T_1 + T_2](q^2)_q$ . (b) Separately extracted  $T_1(q^2)$  and  $T_2(q^2)$  are compared with  $[T_1 + T_2](q^2)$ .  $T_1(0)$  (red square) is from the forward matrix element. (c) Chiral extrapolation of  $T_1(0)$  and  $T_2(0)$  for the  $u/d$  quark. They are not renormalized.



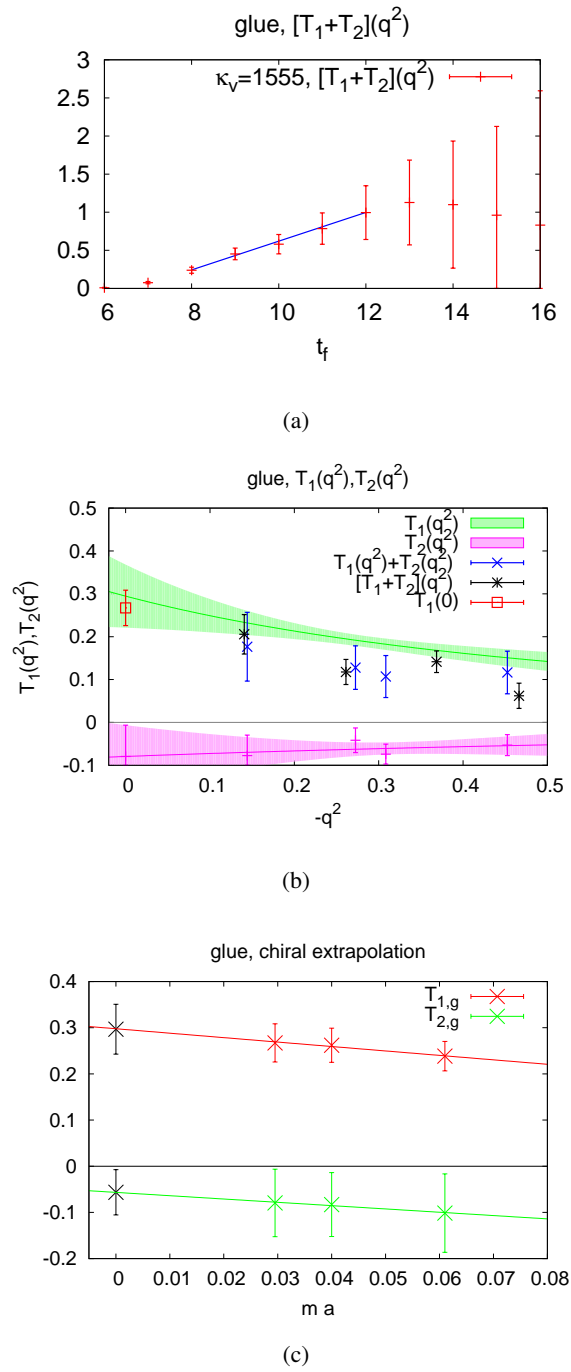


**Figure 3:** The same as in Fig. 2 for the glue.

with light quarks [2, 3, 4]. The large  $2L$  for the  $u/d$  and  $s$  quarks in the DI is due to the fact that  $g_A^0$  in the DI is large and negative, i.e.  $-0.12(1)$  for each of the three flavors. All together, the quark orbital angular momentum constitutes a fraction  $0.50(2)$  of the proton spin. The majority of it comes from the DI. The quark spin fraction of the nucleon spin is  $0.25(12)$  and glue angular momentum contributes a fraction  $0.25(8)$ .

## 5. Summary

In summary, we have carried out a complete calculation of the quark and glue momentum and angular momentum in the nucleon on a quenched  $16^3 \times 24$  lattice with three quark masses. The calculation includes both the connected insertion (CI) and disconnected insertion (DI) of the three-point functions for the quark energy-momentum tensor. We used complex  $Z_2$  (or  $Z_4$ ) noise to estimate the quark loops in the DI and the gauge-field tensor from the overlap operator in the glue energy-momentum tensor. We find that we can obtain reasonable signal for the glue operator constructed from the overlap Dirac operator. After chiral extrapolation, we use the momentum and angular momentum sum rules to determine the lattice renormalization constants which turn out to have a ‘natural’ size close to unity,  $Z_q(a) = 1.05$  and  $Z_g(a) = 1.05$ . The lattice renormalized momentum fractions for the quarks are  $0.586(45)$  for the CI and  $0.100(12)$  for the DI. The glue momentum fraction is  $0.313(56)$ . We have shown that the anomalous gravitomagnetic moment Eq. (2.11) vanishes due to the momentum and angular momentum conservation.

After subtracting from the angular momentum  $2J$  the quark spin ( $g_A^0$ ) from a previous calculation on the same lattice [14], we obtain the orbital angular fraction  $2L$ . In the CI, we find that the  $u$  quark contribution is negative, while the  $d$  quark contribution is positive. The sum is small,  $0.04(9)$ . This behavior is about the same as observed in dynamical calculation with light quarks [2, 3, 4]. The majority of the quark orbital angular momentum comes from the DI, because the quark spin from the DI is large and negative for each of the three flavors. In the end, we find the quark orbital angular momentum, the quark spin, and glue angular momentum fractions of the nucleon spin are  $0.50(2)$ ,  $0.25(12)$ , and  $0.25(8)$  respectively.

We are in the process of calculating the perturbative matching to the  $\overline{\text{MS}}$  scheme with mixing so that we can quote our results in  $\overline{\text{MS}}$  scheme at 2 GeV.

## Acknowledgment

This work is partially support by U.S. DOE Grant No. DE-FG05-84ER40154 and the Center for Computational Sciences of the University of Kentucky. The work of M. Deka is partially supported by the Institute of Mathematical Sciences, India.

## References

- [1] N. Mathur, S. J. Dong, K. F. Liu, L. Mankiewicz, N. C. Mukhopadhyay, Phys. Rev. **D62**, 114504 (2000), [hep-ph/9912289].
- [2] P. Hagler *et al.* [LHPC and SESAM Collaborations], Phys. Rev. **D68**, 034505 (2003). [hep-lat/0304018].

- [3] D. Brommel *et al.*, PoS, **LATTICE2007**, 158 (2007).
- [4] J.D. Bratt *et al.* [LHPC Collaborations], Phys. Rev. **D82**, 094502 (2010).
- [5] M. Stolarski (COMPASS Collaboration), Nucl. Phys. **Proc. Suppl.** **207-208**, 53 (2010); P. Djawotho (STAR Collaboration), J. Phys. Conf. Ser. **295**, 012061 (2011).
- [6] S. Brodsky and S. Gardner, Phys. Lett. **B643**, 22 (2006), [hep-ph/0608219].
- [7] S. Brodsky, D.S. Hwang, B.Q. Ma, I. Schmidt, Nucl. Phys. **B593**, 311 (2001), [hep-th/0003082].
- [8] X. -D. Ji, Phys. Rev. Lett. **78**, 610 (1997), [hep-ph/9603249].
- [9] K. F. Liu, A. Alexandru, I. Horvath, Phys. Lett. **B659**, 773-782 (2008), [hep-lat/0703010].
- [10] K. F. Liu, S. J. Dong, Phys. Rev. Lett. **72**, 1790-1793 (1994), [hep-ph/9306299].
- [11] K. F. Liu, S. J. Dong, T. Draper, D. Leinweber, J. H. Sloan, W. Wilcox, R. M. Woloshyn, Phys. Rev. **D59**, 112001 (1999), [hep-ph/9806491].
- [12] K. F. Liu, Phys. Rev. **D62**, 074501 (2000), [hep-ph/9910306].
- [13] L. Maiani, G. Martinelli, M. L. Paciello, B. Taglienti, Nucl. Phys. **B293**, 420 (1987).
- [14] S. J. Dong, J. -F. Lagae, K. F. Liu, Phys. Rev. Lett. **75**, 2096-2099 (1995), [hep-ph/9502334].
- [15] M. Deka, T. Streuer, T. Doi, S. J. Dong, T. Draper, K. F. Liu, N. Mathur, A. W. Thomas, Phys. Rev. **D79**, 094502 (2009), [arXiv:0811.1779 [hep-ph]].
- [16] T. Doi, M. Deka, S. -J. Dong, T. Draper, K. F. Liu, D. Mankame, N. Mathur, T. Streuer, Phys. Rev. **D80**, 094503 (2009), [arXiv:0903.3232 [hep-ph]].
- [17] S. J. Dong, J. F. Lagae, K. F. Liu, Phys. Rev. **D54**, 5496-5500 (1996), [hep-ph/9602259].
- [18] S. J. Dong, K. F. Liu, Phys. Lett. **B328**, 130-136 (1994), [hep-lat/9308015].
- [19] T. Doi *et al.* [ QCD Collaboration ], PoS **LATTICE2008**, 163 (2008), [arXiv:0810.2482 [hep-lat]].
- [20] C. W. Bernard, Lectures at TASI '89, Boulder, CO, Jun 4-30, 1989, Published in Boulder ASI 1989:233-292.
- [21] T. Draper, R. M. Woloshyn, W. Wilcox, K. F. Liu, Nucl. Phys. **B318**, 319 (1989).
- [22] C. Thron, S. J. Dong, K. F. Liu, H. P. Ying, Phys. Rev. **D57**, 1642-1653 (1998). [hep-lat/9707001].
- [23] H.L. Lai, P. Nadolsky, J. Pumplin, D. Stump, W.K. Tung, C.-P. Yuan, JHEP **0704**, 089 (2007), [hep-ph/0702268].
- [24] H.L. Lai *et al.*, Phys. Rev. **D55**, 1280 (1997).